Water Air Soil Pollut (2013) 224:1552
DOI 10.1007/s11270-013-1552-y

Defluoridation of Groundwater Using Termite Mound

Fekadu Fufa · Esayas Alemayehu · Bernd Lennartz

Received: 12 January 2013 / Accepted: 28 March 2013 / Published online: 17 April 2013

Abstract High concentration of fluoride in groundwater is a longstanding health problem. Fluoride adsorption capacity of termite mound (TM), containing mainly silicon, aluminum, iron, and titanium oxides, was investigated under a batch adsorption system. The influence of parameters such as contact time, solution pH, adsorbent dose, initial fluoride concentration, and the presence of competing anions was investigated. Equilibrium was achieved within 10 min of agitation time. A high percentage (~90 %) of fluoride removal was obtained in a wide pH range 3–8, which is important in the practical application. Kinetics data followed the pseudo-second-order model ($R^2 > 0.99$). The Dubinin–Radushkevich isotherm described most satisfactorily ($R^2 = 0.968$, $\chi^2 = 0.09$) the equilibrium adsorption, giving a sorption capacity of 2.70 mg/g. The obtained mean free energy ($E_{DR} = 11.62$ kJ/mol) suggested that chemisorption should be mainly responsible for fluoride adsorption. Fluoride removal was significantly decreased in the presence of carbonate and phosphate ions, whereas slightly increased in the presence of chloride, nitrate, and sulfate. The adsorbent reduced 7.56 mg/L fluoride content of groundwater to below 1.5 mg/L. The fluoride-loaded TM was successfully regenerated using calcined eggshell or NaOH solution with insignificant loss of metals. The adsorption efficiency of the regenerated TM was comparable to the fresh TM. The results obtained from this study could provide important information for evaluating the application of TM for defluoridation.

Keywords Calcined eggshell · Equilibrium · Kinetics · Regenerable adsorbent

F. Fufa (✉) · B. Lennartz
Faculty of Agricultural and Environmental Sciences,
Rostock University,
Justus-Von-Liebig-Weg 6,
18059 Rostock, Germany
e-mail: fekadufufa@ymail.com

E. Alemayehu · B. Lennartz
Jimma Institute of Technology, Jimma University,
Jimma, Oromia, Ethiopia

1 Introduction

Drinking water has been artificially fluoridated to prevent tooth decay. However, the controversy surrounding the health benefits of fluoride even at low concentrations is rising (Maliyekkal et al. 2008). Health problems associated with the consumption of excess fluoride is growing, and many millions of people across the world are exposed to high fluoride concentrations, mainly from drinking groundwater (WHO 2006). The problem is severe in China, India, Sri Lanka, and countries in the East African Rift Valley, including Ethiopia (Jagtap et al. 2012). Drinking groundwater sources in the Main Ethiopian Rift contain fluoride as high as 23 mg/L (Rango et al. 2010; Furi et al. 2011). The World Health Organization (WHO) set a guideline value for fluoride concentration in drinking water to 1.5 mg/L (WHO 2006). However, the guideline is not universal.

Various defluoridation technologies such as membrane techniques, application of different chemicals, and adsorption methods have been used for the removal

of fluoride. The membrane methods, which effectively reduce fluoride concentration to acceptable levels, include reverse osmosis, dialysis, nanofiltration, and electrodialysis (Mohapatra et al. 2009). The techniques are, however, complex, require skilled labor, and have high initial and maintenance costs (Bhatnagar et al. 2011). Likewise, defluoridation using various chemicals is complex, uneconomical, and requires skilled labor and chemical handling (Chauhan et al. 2007). These drawbacks hinder the implementation of the membrane and chemical defluoridation technologies in the fluorosis endemic regions of developing countries like Ethiopia.

Many researchers have been working to come up with simple, low-cost, and effective adsorbents, and to improve the efficiency of the adsorbents. Thus, various natural, modified, and synthetic adsorbents such as soils (Wang and Reardon 2001), bauxite (Das et al. 2005), laterite (Sarkar et al. 2006), iron(III)-loaded ligand cotton (Zhao et al. 2008), hydrous iron(III)–tin(IV) bimetal mixed oxide (Biswas et al. 2009), titanium modified chitosan (Jagtap et al. 2009), granular ferric hydroxide (Kumar et al. 2009), granular red mud (Tor et al. 2009), granular ceramic (Chen et al. 2011a), allophane (Kaufhold et al. 2010), bone char (Ramos et al. 2010), iron- and aluminum-based mixed hydroxide (Sujana and Anand 2010), cellulose fibers (Tian et al. 2011) and many others have been investigated. The practical applicability of the low-cost adsorbents is limited either due to their low efficiency or cultural taboo. Hence, studies have been going on to explore a simple, low-cost, efficient, and socially acceptable adsorbent. However, termite mound (TM) that is abundant in nature has not been investigated for the removal of fluoride. Therefore, the present study aimed (1) to evaluate the fluoride sorption capacity of TM under batch adsorption setup; (2) to assess trends of fluoride adsorption with respect to variation of contact time, solution pH, adsorbent dose, initial fluoride concentration, and initial concentration of co-existing anions; and (3) to examine the regenerative properties of the fluoride-loaded adsorbent.

2 Materials and Methods

2.1 Adsorbent

Termite hills are built by mound-building termites that significantly modify the physicochemical properties of soil (Jouquet et al. 2002; Semhi et al. 2008). Mounds are widely distributed and abundant in nature (Jouquet et al. 2002; Lopez-Hernandez et al. 2006; Semhi et al. 2008). In Ethiopia, TMs are abundantly found. In the southern and western parts of Ethiopia, average mound abundance is found to be 12 mounds per hectare (Abdulrahman 1990; Tilahun et al. 2012), and the average mound soil mass is estimated to be 58.9 tons per hectare (Tilahun et al. 2012). In the western part of Ethiopia, in eight districts of the east and west Wellega zones, infestation of mound-building termites has been a serious problem for the local community (OADB 2001). Samples of mound soil were collected from six TMs in the surroundings of Gimbi, west Wellega Zone, Oromia Regional National State, western Ethiopia. The rocks of the sampling area are Precambrian formations comprising a wide range of sedimentary, volcanic, and intrusive rocks that have been metamorphosed to varying degrees (Tadesse et al. 2003). A composite sample was made mixing thoroughly the six samples in a 1:1 ratio, and dried afterwards at room temperature in a laboratory. Particle size analysis of the composite sample was performed according to the American Society for Testing and Materials (ASTM D 422) and soil textural classification system (Liu and Evett 2003). The dried sample was crushed by hand in a mortar, and sieved to <0.075-mm particle size. Then the sieved sample was packed in an air-tight plastic bottle for later investigation. The moisture content was determined by heating in an oven at 105 °C for 24 h. The pH of the adsorbent was measured using a Microprocessor pH meter (pH 196, WTW, Germany) at a 1:10 TM/water ratio according to the standard method (Appel and Ma 2002). The pH of the point of zero charge (pH_{PZC}) was determined by the potentiometric titration method (Appel et al. 2003). Major oxide and some minor elemental compositions of the composite sample were analyzed using X-ray fluorescence (XRF) spectrometry and inductively coupled plasma (ICP) spectrometer (Thermo Scientific iCAP 6300 ICP, Thermo Fischer Scientific, Cambridge, UK), respectively. The total carbon, total nitrogen, and total sulfur contents were determined using Elementar Vario EL analyser (Elementar Analysensysteme GmbH, Hanau, Germany) according to DIN ISO 10694 and 13878 (DIN 1996, 1998). The specific surface area of the adsorbent of particle size <0.075 mm was determined by BET method using Micromeritics (ASAP 2010, USA) after degassing.

2.2 Chemicals

All the chemicals used were analytical grade reagents from Merck, Darmstadt, Germany. A 1,000-mg/L fluoride stock solution was prepared by dissolving 2.21 g anhydrous NaF in 1 L of deionized water. Working solutions of fluoride were prepared by appropriately diluting the stock solution. Potassium salts of bicarbonate, carbonate, chloride, nitrate, phosphate, and sulfate anions were used in the investigation of the effects of competing anions. Solution of sodium bicarbonate and sodium carbonate was used as eluent, and sulfuric acid was used as a chemical suppressant in the Metrohm ion chromatography system. The pH of solution was adjusted using 0.1 M NaOH and/or 0.1 M HCl.

2.3 Preparation of Desorbent

Eggshell calcined in a furnace at 900 °C for 3 h contains ~97 % calcium oxide (Thongthai 2011). Accordingly, to prepare calcium oxide from eggshell, eggs were bought from Aldi supermarket, Rostock, Germany. The inner soft part of the raw eggshell was carefully peeled off. Then the external hard shell was washed with deionized water and dried in an oven at 105 °C for 24 h. The dried eggshell was milled by hand in a mortar for calcination at 900 °C for 3 h in a preheated furnace (Balázsi et al. 2007; Gergely et al. 2010) and afterward cooled in a desiccator. To prepare an alkaline solution of $Ca(OH)_2$, 200 g of the powder of calcined eggshell was stirred in 1 L deionized water and filtered to remove undissolved matter. Then the supernatant solution of $Ca(OH)_2$ labeled "CES solution" having pH 12.70 was used for fluoride desorption.

2.4 Adsorption Experiments

Sets of batch adsorption experiments were conducted to understand the fluoride adsorption process of TM under various experimental conditions. In all sets of the experiments, a known concentration of fluoride and a desired amount of TM were mixed in 500 mL solution in acid-washed polyethylene plastic bottles and agitated for 60 min at 200 rpm on a horizontal shaker (SM25, Edmund Bühler 7400 Tübinger, Germany). All the experiments were in duplicate at room temperature (23.5–25.5 °C), and the results reported were the averages. Blank (only with TM) and control (only with fluoride) experiments were conducted at every set of the experiments.

Throughout the study, particle size of <0.075 mm, 10 mg/L fluoride concentration (except in the study of the effect of initial fluoride concentration), 30 g/L of TM (except in the investigation of the effect of adsorbent dose), and solution pH ~ 7 (except in the study of the effect of solution pH) were used. Ten-milliliter supernatant solutions were drawn at desired time intervals (0–60 min). The pH of the solution was measured by a Microprocessor pH meter (pH 196, WTW, Germany) before the analysis of residual fluoride. The supernatant solution samples were then filtered with 0.45-μm acetate filter paper (Sartorius Stedim Biotech GmbH, Germany) for the analysis of residual fluoride.

The effect of contact time was investigated using 30 g/L TM in 500 mL solution of 10 mg/L fluoride. The influence of solution pH was investigated by adjusting the initial pH from 3 to 11 and keeping the other parameters constant. The effect of the adsorbent dose was studied by varying the amount of the adsorbent from 1 to 100 g/L under the initial fluoride concentration of 10 mg/L. Kinetics of fluoride adsorption was examined using three different adsorbate/adsorbent ratios: 10 mg F^-/8 g TM, 20 mg F^-/15 g TM, and 50 mg F^-/30 g TM. The influence of initial concentration of fluoride was examined by varying the concentration from 3 to 155 mg/L and maintaining the other experimental conditions constant. The effect of the presence of competing anions (bicarbonate, carbonate, chloride, nitrate, phosphate, and sulfate) in the solution separately or in a mixture on the removal of fluoride was investigated under a fixed fluoride concentration of 10 mg/L while varying the initial concentration of the anions from 10 to 500 mg/L.

The percentage of fluoride removed, $A\%$, and the amount of fluoride adsorbed per unit mass of the adsorbent, q_t (milligrams per gram), at any time t (minutes) are computed respectively using Eq. 1 and Eq. 2 given below:

$$A\% = \left(\frac{C_0 - C_t}{C_0}\right) \times 100 \tag{1}$$

$$q_t = \left(\frac{C_0 - C_t}{m}\right) \times V \tag{2}$$

where C_0 (milligrams per liter) is the initial concentration of fluoride in the solution, C_t (milligrams per liter) is the concentration of fluoride in the aqueous phase at any time, t (minutes), V (liters) is the volume of the solution, and m (grams) is the mass of the adsorbent.

2.5 Desorption–Adsorption Study

The regeneration of an adsorbent basically depends on the ease with which an adsorbate is released from the spent adsorbent. For fluoride desorption experiments, fluoride-loaded adsorbent was prepared by agitating 30 g/L of the adsorbent with 10 mg/L fluoride at 200 rpm for 60 min at pH ~ 7. After adsorption, the solid was separated from the supernatant solution by filtration. The solid on the filter paper was washed with deionized water. The fluoride-loaded TM was dried at 105 °C for 12 h in an oven. Desorption experiments were carried out by shaking the oven-dried spent TM at 200 rpm for 60 min in 500-mL CES, 0.1 and 0.2 M NaOH solution separately. To assess the safe disposal of the fluoride-loaded TM at pH ≤ 5, the pH of deionized water was adjusted to ~5 to be used as a desorbent solution. The amount of fluoride desorbed was determined via the analysis of fluoride in the supernatant solution. After desorbing fluoride from the fluoride-loaded TM, the TM was rinsed with 0.1 M HCl solution until the pH of the supernatant solution was ~5, which was the pH of the fresh TM sample determined at 1:10 TM/water ratio. Then the regenerated TM was dried at room temperature for 7 days. To examine the adsorption efficiency of the regenerated adsorbent, the dried reactivated TM was put in contact with 10 mg/L fluoride for 60 min at a solution pH ~ 7.

2.6 Analysis

The concentration of fluoride was analyzed by ion chromatography (Metrohm AG, Switzerland) with chemical suppression and a Metrosep Dual 2 column (75 mm). Calibration of the ion chromatography using fluoride standard solution was performed at each set of the analysis. Fluoride concentration was calculated on the basis of the peak area using a quadratic regression equation derived from the measurements of the standard solutions. Dissolution of the adsorbent under equilibrium experimental conditions (shaking speed 200 rpm, contact time 60 min, pH ~ 7, and temperature 23.7 °C) was investigated via the analysis of the concentrations of elements using inductively coupled plasma (ICP) spectrometer (Thermo Scientific iCAP 6300 ICP, Thermo Fischer Scientific, Cambridge, UK).

2.7 Data Analysis

2.7.1 Adsorption Kinetics

The adsorption kinetics of the system can be explained by the pseudo-second-order equation (Eq. 3) when the removal of an adsorbate from aqueous solution increases during the initial agitation time, and followed by a slow increase until the equilibrium time (Ho and McKay 1999).

$$\frac{dq_t}{dt} = k_2(q_e - q_t)^2 \tag{3}$$

where q_t (milligrams per gram) is the amount of fluoride adsorbed per unit mass of the adsorbent at any time t (minutes), q_e (milligrams per gram) is the calculated equilibrium capacity, and k_2 (grams per milligram per minute) is the equilibrium rate constant based on the pseudo-second-order equation. Integrating Eq. 3 for the boundary conditions $q_t = 0$ to $q_t = q_t$ at $t = 0$ to $t = t$ is simplified and linearized to obtain Eq. 4.

$$\frac{t}{q_t} = \frac{1}{k_2 q_e^2} + \frac{1}{q_e}(t) \tag{4}$$

The values of k_2 and q_e were calculated from the intercept and the slope of the plot of t/q_t versus t, respectively.

2.7.2 Adsorption Isotherms

To evaluate the fluoride sorption capacity of TM, the relationship between the amount of fluoride adsorbed at equilibrium per unit mass of the adsorbent and the concentration of fluoride in the aqueous phase at equilibrium was analyzed by applying adsorption isotherm models. The nonlinear forms of the three widely used isotherms (Sujana et al. 1998; Nigussie et al. 2007; Tripathy and Raichur 20088; Sarı and Tuzen 2009; Solangi et al. 2009), namely, the Langmuir (Eq. 5), the Freundlich (Eq. 6), and the Dubinin–Radushkevich (D–R; Eq. 7) equations, were used to estimate the

fluoride adsorption capacity of the adsorbent.

$$q_e = \frac{Q_{max} b C_e}{(1 + bC_e)} \quad (5)$$

$$q_e = K_F C_e^{\frac{1}{n}} \quad (6)$$

$$q_e = q_m \exp\left(-K_{DR}\varepsilon^2\right) \quad (7)$$

$$\varepsilon = RT \ln\left(1 + \frac{1}{C_e}\right) \quad (8)$$

where C_e (milligrams per liter) is the concentration of fluoride in the aqueous phase at equilibrium, q_e (milligrams per gram) is the amount of fluoride adsorbed at equilibrium per unit mass of TM, Q_{max} (milligrams per gram) is the adsorption capacity based on the Langmuir equation, and b (liters per milligram) is the Langmuir constant, K_F (liters per gram) is the adsorption capacity based on the Freundlich equation, $1/n$ is the adsorption intensity based on the Freundlich equation, q_m (moles per gram) is the molar adsorption capacity based on the D–R equation, K_{DR} (square moles per square kilojoules) is the activity coefficient related to the mean sorption energy, ε (square moles per square kilojoules) is the Polanyi potential, R (kilojoules per mole per Kelvin) is the gas constant, and T (Kelvin) is the temperature of the equilibrium experiment.

The mean sorption energy, E_{DR} (kilojoules per mole), can be computed by Eq. 9 using the value of K_{DR} obtained from the D–R model.

$$E_{DR} = -(-2K_{DR})^{-0.5} \quad (9)$$

The value of E_{DR} is important to estimate the type of adsorption reaction. When the value of E_{DR} ranges from 8.0 to 16.0 kJ/mol, the sorption reaction should be chemisorption, and when E_{DR} < 8.0 kJ/mol, the adsorption process can be physical sorption (Biswas et al. 2009). The separation factor, R_L, of the Langmuir isotherm, which is a dimensionless constant, was computed applying Eq. 10 (Meenakshi et al. 2008).

$$R_L = \frac{1}{1 + bC_0} \quad (10)$$

where C_0 (milligrams per liter) is the initial fluoride concentration. The value of R_L is useful in determining the type of the isotherm. Accordingly, the isotherm is irreversible ($R_L = 0$), favorable ($0 < R_L < 1$), linear ($R_L = 1$), or unfavorable ($R_L > 1$; Meenakshi et al. 2008).

To identify a suitable isotherm model for the sorption of fluoride on TM, a Chi-squared analysis was carried out (Meenakshi et al. 2008). The mathematical statement of the Chi-squared test statistic is given by Eq. 11.

$$\chi^2 = \sum \frac{\left(q_e - q_{e,cal}\right)^2}{q_{e,cal}} \quad (11)$$

where $q_{e,cal}$ (milligrams per gram) is the equilibrium capacity obtained by calculation from the model, and q_e (milligrams per gram) is the experimental data on the equilibrium capacity. If data from the model are similar to the experimental data, χ^2 will be a small number; while if they differ, χ^2 will be a bigger number (Meenakshi et al. 2008). Therefore, it is necessary to analyze the data set using the nonlinear Chi-squared test to confirm the isotherm that best describes the sorption system.

3 Results and Discussion

3.1 Characterization of the Adsorbent

The analyzed results of chemical composition of TM are given in Table 1. It is interesting to note that the iron, aluminum, and titanium oxides are significantly high and together amounted to 57.77 wt.%, whereas the sum of the content of basic metallic oxides (sodium, calcium, magnesium, and potassium oxides) of the adsorbent was negligible (~1 wt.%). The elemental content of Si, Fe, Al, and Ti together added up to 35.59 wt.%. Concentrations of the analyzed toxic elements were below their respective detection limit except for chromium, which was 0.01 wt.%. The total carbon, total sulfur, and total nitrogen content of the sample together constituted 2.62 wt.%. The pH of the adsorbent measured in water was 5.10, and moisture content was 3.92 %. The pH_{PZC} of TM determined by the potentiometric titration method was found to be 7.96. The obtained value of pH_{PZC} is within the range of the pH_{PZC} of the mixture of Si, Fe, Al, and Ti oxides, 5.5 to 8.3 (Brown et al. 1998), and comparable to the pH_{PZC} of TM (pH_{PZC} = 7.8) investigated for the removal of Pb(II) (Abdus-Salam and Itiola 2012). Particle size analysis showed that majority of the particles was in the

Table 1 Chemical compositions of TM

Oxides/elements	wt.%	Elements	wt.%
SiO_2	27.43	Si	15.07
Al_2O_3	22.83	Fe	12.67
Fe_2O_3	26.08	Al	6.35
TiO_2	8.86	Ti	1.50
MgO	0.83	Na	<0.01
Na_2O	<0.01	K	<0.01
K_2O	0.23	Mg	<0.01
CaO	<0.01	Cr	0.01
MnO	0.25	Mn	0.21
P_2O_3	0.35	P	0.35
SO_3	0.33	Hg	bdl
LOI	11.29	Pb	bdl
Total C	2.30	As	bdl
Total S	0.28	Ni	bdl
Total N	0.04	Cd	bdl

LOI loss on ignition, *bdl* below detection limit

range of 0.075–2.00 mm with mean particle size (d_{50}) of 0.51 mm. The BET surface area of TM of particle size <0.075 mm was found to be 28.4 m^2/g.

3.2 Solubility of TM

An investigation was carried out to assess the solubility of TM and the release of some toxic elements under the equilibrium experimental conditions (shaking speed 200 rpm, contact timer 60 min, solution pH ~ 7, and temperature 24.6 °C). Mineral dissolution was tested via the analysis of the concentrations of elements in the supernatant solution. The analyzed data (weight percent) are Si (3.21×10^{-3}), Fe (3.45×10^{-3}), Al (4.97×10^{-3}), As (bdl), Ni (7.33×10^{-6}), Cd (bdl), Cr (7.00×10^{-6}), Pb (bdl), F (6.67×10^{-6}), Cl (9.45×10^{-3}), NO_3^- (1.13×10^{-3}), and SO_4^{2-} (1.12×10^{-2}), where bdl is below the detection limit. The results indicated that the dissolution of TM was insignificant, and the concentrations of elements obtained were significantly lower than their maximum permissible level of WHO (WHO 2006) in drinking water. Therefore, TM can be used safely as an adsorbent for the removal of fluoride.

3.3 Effect of Contact Time

The effect of agitation time was investigated by varying the contact time from 0 to 60 min under 10 mg/L fluoride concentration at pH ~ 7. Figure 1 shows the plot of the percentage of fluoride adsorbed versus the contact time. The result showed that the amount adsorbed was initially fast within the first 5 min of contact time at which ~87 % fluoride was adsorbed. The rapid adsorption of fluoride in the first 5 min of the agitation time was due to the presence of free active binding sites on the surface of the adsorbent at the initial stage of the contact time. Equilibrium was achieved within 10 min of the agitation time at which ~90 % fluoride was adsorbed. However, to ensure the attainment of the equilibrium, the agitation time was maintained at 60 min for each set of the experiments.

3.4 Adsorption Kinetics of Fluoride

The kinetics of fluoride adsorption on TM was investigated using three adsorbate/adsorbent ratios (10 mg F^-/8 g TM, 20 mg F^-/15 g TM, and 50 mg F^-/30 g TM or 1.25, 1.33, and 1.67 mg/g, respectively) agitated for 60 min at pH ~ 7. The linear plots of the pseudo-second-order fluoride sorption kinetics are given in Fig. 2, and the values of k_2, $q_{e,cal}$ (calculated), and $q_{e,exp}$ (experimental) are reported in Table 2. The analysis of the kinetics data showed that the values of the coefficient of determination $R^2 > 0.99$ for each plot. Moreover, the values of $q_{e,cal}$ (calculated) and $q_{e,exp}$ (experimental) were nearly equal. Therefore, it could be concluded that the adsorption of fluoride on TM followed the pseudo-second-order kinetics equation, suggesting that chemisorption could be

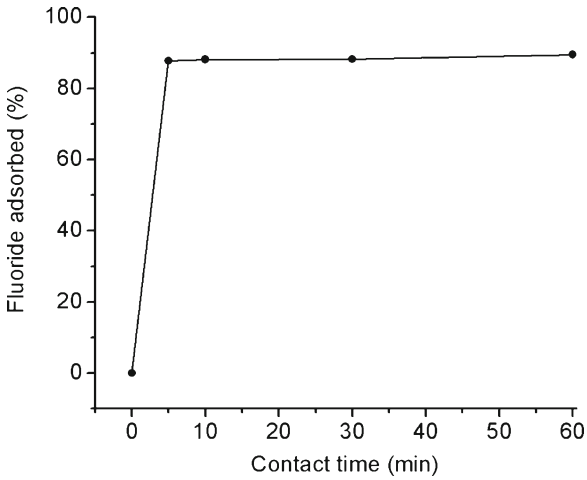

Fig. 1 Effect of contact time on the removal of fluoride by TM ($[F^-]_{initial}$, 10 mg/L; dose, 30 g/L; $pH_{initial}$, ~7; grain size, <0.075 mm; volume of solution, 0.5 L; contact time, 60 min; and shaking speed, 200 rpm)

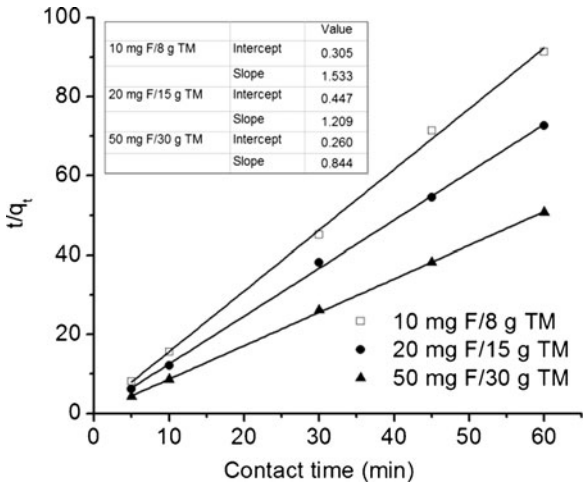

Fig. 2 Pseudo-second-order plots of fluoride adsorption kinetics ($[F^-]_{initial}$, 10 mg/L; adsorbate/adsorbent ratio, 10 mg F^-/8 g TM, 20 mg F^-/15 g TM, and 50 mg F^-/30 g TM; $pH_{initial}$, ~7; grain size, <0.075 mm; volume of solution, 0.5 L; contact time, 60 min; and shaking speed, 200 rpm)

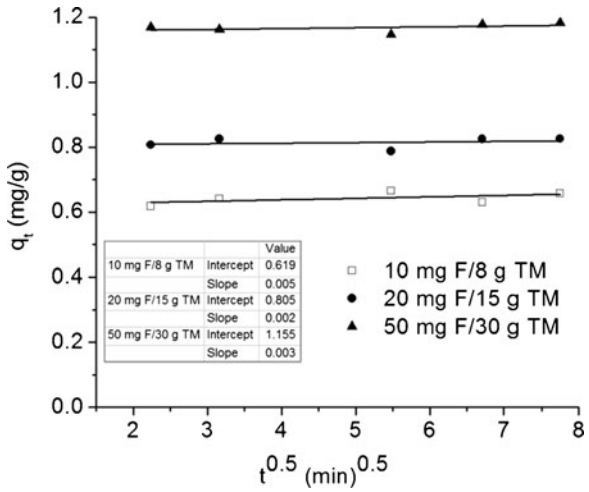

Fig. 3 Intraparticle diffusion plots of fluoride adsorption kinetics ($[F^-]_{initial}$, 10 mg/L; adsorbate/adsorbent ratio, 10 mg F^-/8 g TM, 20 mg F^-/15 g TM, and 50 mg F^-/30 g TM; $pH_{initial}$, ~7; grain size, <0.075 mm; volume of solution, 0.5 L; contact time, 60 min; and shaking speed, 200 rpm)

the main process of fluoride adsorption (Camacho et al. 2010). The pseudo-second-order rate constant, k_2, decreased with the increase in the adsorbate/adsorbent ratio, indicating that the higher the concentration, the faster the adsorption (Lucy et al. 2010).

The diffusion mechanism of fluoride molecules was examined by applying the Morris and Weber intraparticle diffusion model (Sujana et al. 1998; Nigussie et al. 2007) that is given by $q_t = k_p t^{0.5}$, where k_p (milligrams per gram per the square root of minute) is the intraparticle diffusion rate constant. If there is intraparticle diffusion, a linear relation between the amount of fluoride adsorbed and the square root of time will be observed. The values of the intraparticle diffusion rate constant computed from the plots of q_t versus $t^{0.5}$ are given in Table 2. Figure 3 shows the adsorption capacity of TM at different adsorbate/adsorbent ratios as a function of a square root of time. The plots show that a linear relationship was not observed ($R^2 > 0.50$) between the amount of fluoride adsorbed and the square root of time, indicating that film diffusion may not be the rate-limiting step (Sujana et al. 1998; Nigussie et al. 2007). Hence, the result supported the fast equilibrium time. The result is in good agreement with the similar work done by Nigussie et al. (2007) using waste residue from alum manufacturing process.

3.5 Effect of Adsorbent Dose

The effect of adsorbent dose on the removal of fluoride was studied by varying the amount of TM from 1

Table 2 Pseudo-second-order and intraparticle diffusion constants for fluoride adsorption at different adsorbate/adsorbent ratios

Model	Parameter	Adsorbate/adsorbent ratio		
		10 mg F^-/8 g TM	20 mg F^-/15 g TM	50 mg F^-/30 g TM
Pseudo-second-order	$q_{e,exp}$ (mg/g)	0.657	0.826	1.183
	$q_{e,cal}$ (mg/g)	0.652	0.827	1.185
	k_2 [g/(mg.min)]	7.705	3.270	2.740
	R^2	0.9983	0.9989	0.9996
Intraparticle diffusion	k_p [mg/(g.min$^{0.5}$)]	0.005	0.002	0.003
	C (mg/g)	0.619	0.805	1.155
	R^2	0.3135	0.0631	0.1806

to 100 g/L and keeping the other experimental conditions constant. The percentage of fluoride adsorbed and fluoride adsorption capacity at different TM doses are given in Fig. 4. According to the results obtained, the percentage of fluoride adsorbed increased from ~13 % to ~99 % with the increase in the adsorbent dose from 1 to 100 g/L. The increase in the adsorption with the adsorbent dosage can be attributed to the greater surface area and the availability of more adsorption sites at a higher adsorbent dosage (Chen et al. 2011a). On the other hand, the amount of fluoride adsorbed decreased from ~1.56 to ~0.12 mg/g with the increase in the adsorbent dose. The decrease in the adsorption capacity was possibly due to the lower ratio of fluoride ions to the available active binding sites with increasing mass of the adsorbent (Thole 2011). Fluoride removal increased significantly up to the adsorbent dose of 30 g/L, which adsorbed ~90 % of 10 mg/L fluoride in the solution. However, no significant increase in the percentage of fluoride removal was observed beyond 30 g/L TM. The 30-g/L dose of the adsorbent was sufficient to decrease 10 mg/L fluoride to below the WHO guideline value of 1.5 mg/L fluoride. Therefore, 30 g/L TM was fixed as the optimum dose, and the rest of the batch adsorption studies were conducted using 30 g/L TM.

The coefficient of distribution, K_D (liter per gram), which shows the binding ability of the adsorbent surface, was calculated using $K_D = q_e/C_e$ (Chen et al. 2011a; Sujana et al. 1998), where C_e (milligram per liter) and q_e (milligram per gram) are defined in Section 2.7.2. The value of the coefficient of distribution depends mainly on the pH and the nature of the adsorbent surface. The K_D value for the adsorption of fluoride on TM increased with the increase in the adsorbent dose at pH ~ 7 (Fig. 5), which is similar to the observation made by Chen et al. (2011a) for the removal of fluoride by ceramic-containing dispersed aluminum and iron oxides. If the surface is homogeneous, the K_D value should not change with an increase in the adsorbent dose at constant pH, so the increase in K_D value in the present study indicated the heterogeneous nature of the surface of TM (Tripathy and Raichur 2008; Chen et al. 2011a).

3.6 Effect of Solution pH

The effect of pH on the removal of fluoride was examined in the initial solution pH ranging from 3 to 11 using 10 mg/L fluoride and 30 g/L TM. The result (Fig. 6) showed that the percentage of fluoride adsorbed was high (~90 %) in the pH range 3–8, which is important in the practical application. However, the percentage significantly decreased from ~88 % to ~45 % upon increasing the pH > 10. It was also observed that fluoride adsorption capacity of TM was almost constant (~0.35 mg/g) in the pH range from 3 to 8, while the amount adsorbed decreased from ~0.34 to ~0.18 mg/g with the increase in the initial pH > 10. The wide pH range for the adsorption of fluoride could be attributed to the amphoteric nature of oxides of aluminum and iron (Shriver et al. 1994;

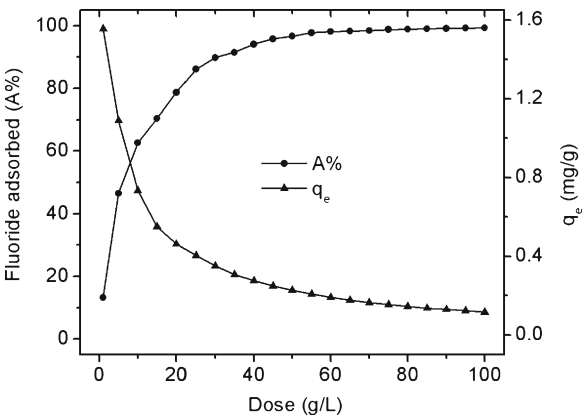

Fig. 4 Effect of adsorbent dose on fluoride removal by TM ($[F^-]_{initial}$, 10 mg/L; dose, 1–100 g/L; $pH_{initial}$, ~7; grain size, <0.075 mm; volume of solution, 0.5 L; contact time, 60 min; and shaking speed, 200 rpm)

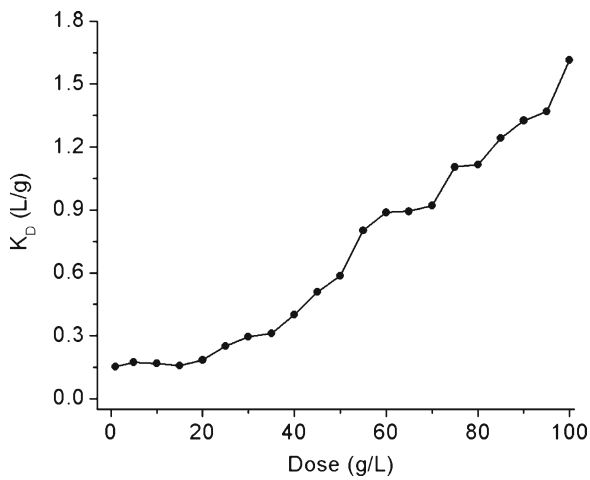

Fig. 5 K_D plot as a function of adsorbent dose ($[F^-]_{initial}$, 10 mg/L; dose, 1–100 g/L; $pH_{initial}$, ~7; grain size, <0.075 mm; volume of solution, 0.5 L; contact time, 60 min; and shaking speed, 200 rpm)

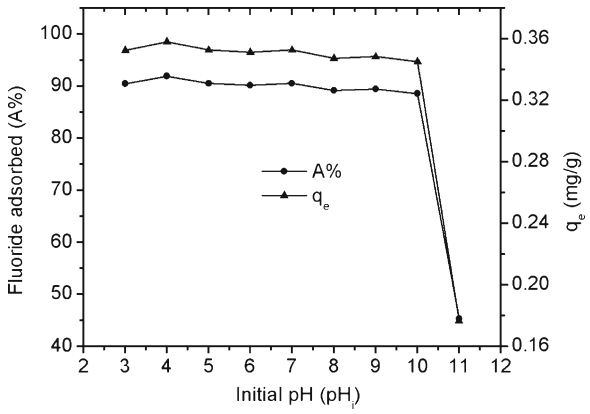

Fig. 6 Effect of solution pH on the removal of fluoride by TM ($[F^-]_{initial}$, 10 mg/L; dose, 30 g/L; $pH_{initial}$, 3–11; grain size, <0.075 mm; volume of solution, 0.5 L; contact time, 60 min; and shaking speed, 200 rpm)

Cornell and Schwertmann 1996; Guo et al. 2007; Liu et al. 2010). The pH dependency of fluoride removal can be explained also considering the pH_{pzc} of the adsorbent. When the pH < pH_{pzc}, the fluoride ions would be adsorbed on the surface of adsorbent by the columbic attraction (Eq. 12), and when the pH > pH_{pzc}, the adsorption of fluoride ions could take place through a ligand exchange process shown in Eqs. 13 and 14 (Ayoob and Gupta 2009).

$$\equiv MOH_2^+ + F^- \Leftrightarrow \equiv MOH_2^+ \cdots F^- \quad (12)$$

$$\equiv MOH + F^- \Leftrightarrow \equiv MF + OH^- \quad (13)$$

$$\equiv MOH_2^+ + F^- \Leftrightarrow \equiv MF + H_2O \quad (14)$$

where M represents Si, Al, Fe, Ti, etc. The decrease in the adsorption of fluoride at pH > 10 could be due to the competition of hydroxyl ions for the adsorption sites with the fluoride ions or electrostatic repulsion of fluoride ion by the negatively charged surface (Chen et al. 2011b). In the pH range from 3 to 8, the fluoride removal efficiency slightly fluctuated, which may be due to both specific and nonspecific adsorption of fluoride onto the adsorbent (Chen et al. 2011b).

Moreover, in this study, the pH of the equilibrated solution increased in the highly acidic pH, and it decreased in the basic medium. Consequently, when the initial solution pH was in the range of 4–10, the pH values after adsorption were ~6.0 (data not shown), implying that the adsorbent had the capacity of maintaining a neutral pH after adsorption. The capacity of the adsorbent to maintain a neutral solution pH after defluoridation may result from two reasons: firstly, the amphoteric nature of aluminum and iron oxides (Shriver et al. 1994; Cornell and Schwertmann 1996), and secondly, the negligible compositional content of basic ionic metallic oxides.

Oxides of iron and aluminum being amphoteric behave as a base in an acidic medium (Eq. 15) and as an acid in a basic medium (Eq. 16; Shriver et al. 1994). The reaction in Eq. 15 shows the decrease in the pH of the medium because the iron and aluminum oxides reduce the $[OH^-]$ in water, whereas these oxides of iron and aluminum diminish the $[H_3O^+]$ in an acidic medium (Eq. 16) resulting in the increase of pH. In addition, covalent oxide contents of the adsorbent, SO_3 and P_2O_3, in the aqueous environment release H_3O^+ to the solution by binding H_2O molecules, resulting in the decrease of the pH of the medium as shown in Eqs. 17 and 18 (Shriver et al. 1994). Thus, iron and aluminum oxides and the covalent oxide contents of TM (Table 1) decreased the equilibrium pH of the solution in synergy.

$$M_2O_{3(s)} + 6H_3O^+_{(aq)} + 3H_2O_{(l)} \Leftrightarrow 2\left[M(OH)_2\right]^{3+} \quad (15)$$

$$M_2O_{3(s)} + 2OH^-_{(aq)} + 3H_2O_{(l)} \Leftrightarrow 2\left[M(OH)_4\right]^-_{(aq)} \quad (16)$$

$$SO_{3(aq)} + H_2O_{(l)} \Leftrightarrow \left[O_2S(OH)_2\right]_{(aq)} \quad (17)$$

$$\left[O_2S(OH)_2\right]_{(aq)} + H_2O_{(l)} \Leftrightarrow [O_3S(OH)]^-_{(aq)} + H_3O^+_{(aq)} \quad (18)$$

where M represents Fe and Al. A recap of the compositional contents of Al_2O, Fe_2O_3, Na_2O, K_2O, CaO, and MgO in the TM given in Table 1 shows that the weight percentage of $Al_2O + Fe_2O_3$ (~49 %) is significantly greater than the percentage of $Na_2O + K_2O +$ CaO + MgO (~1 wt.%); as such, the effect of basic ionic metallic oxides to increase the pH of the solution was negligible and overshadowed by the effect of the amphoteric nature of oxides of aluminum and iron. The result of the influence of pH on the removal of fluoride by TM is similar to previous studies examining the removal of fluoride by granular ceramic-containing dispersed aluminum and iron oxides (Chen

et al. 2011a), ceramic (Chen et al. 2010a), Mg-incorporated bentonite clay (Thakre et al. 2010), and waste residue from alum manufacturing (Nigussie et al. 2007).

3.7 Effect of Initial Concentration of Fluoride and Adsorption Isotherm

The effect of initial concentration of fluoride was assessed by varying the concentration from 3 to 155 mg/L at pH ~ 7 using 30 g/L TM. The percentage of fluoride adsorbed and fluoride adsorption capacity at various initial concentrations of fluoride are presented in Fig. 7. The results indicated that fluoride adsorption capacity increased with the increase in the initial fluoride concentration, whereas the percentage of fluoride removal decreased. The increase in the adsorption capacity could be due to the availability of more fluoride ions at higher fluoride concentration for adsorption on poorly reachable sites with weak sorption energy (Nigussie et al. 2007; Sakhare et al. 2012).

The isotherm plots of the equilibrium adsorption of fluoride are graphically presented in Fig. 8, and the values of the equilibrium constants computed from the isotherm models are given in Table 3. The isotherm model that best describes the fluoride–TM adsorption system was determined by evaluating the values of the coefficient of determination, R^2, and Chi-squared test, χ^2. Accordingly, the D–R isotherm had the highest R^2 and the smallest χ^2 values (Meenakshi et al. 2008), indicating that the model most satisfactorily described the sorption of fluoride on the adsorbent. The fluoride

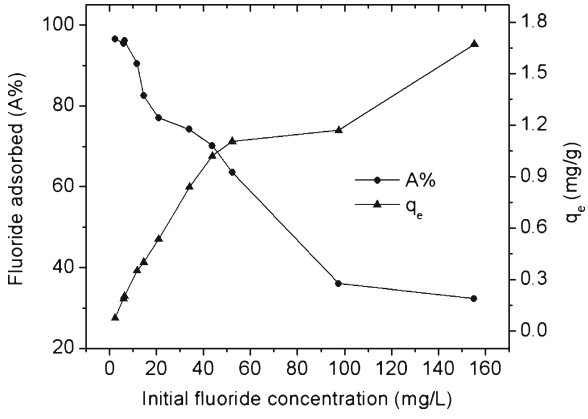

Fig. 7 Effect of initial fluoride concentration on the removal of fluoride by TM ($[F^-]_{initial}$, 3–155 mg/L; dose, 30 g/L; $pH_{initial}$, ~7; grain size, <0.075 mm; volume of solution, 0.5 L; contact time, 60 min; and shaking speed, 200 rpm)

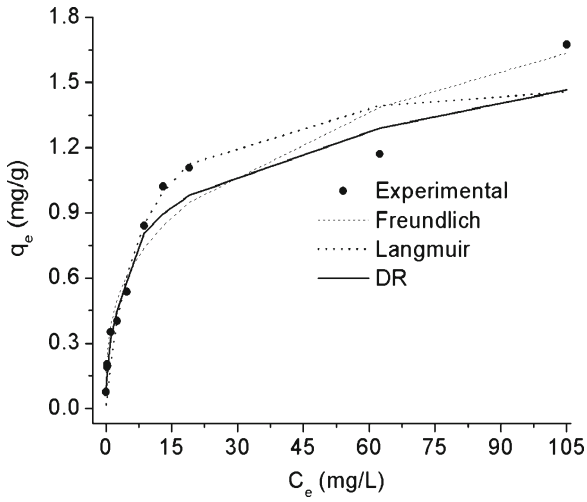

Fig. 8 Isotherms of the equilibrium adsorption of fluoride on TM ($[F^-]_{initial}$, 3–155 mg/L; dose, 30 g/L; $pH_{initial}$, ~7; grain size, <0.075 mm; volume of solution, 0.5 L; contact time, 60 min; and shaking speed, 200 rpm)

sorption capacity of TM obtained at equilibrium from the D–R model was 2.70 mg/g. The computed value of the intensity of fluoride adsorption (n=2.70) was in the range of 1–10, indicating the favorable adsorption of fluoride ions (Solangi et al. 2009). Moreover, the values of R_L calculated using Eq. 9 were from 0.07 to 0.86, verifying the favorable adsorption of fluoride on the adsorbent. The value of the mean sorption energy (E_{DR} = 11.62 kJ/mol) computed from the K_{DR} value using Eq. 10 was within the range of 8.0–16.0 kJ/mol, substantiating the fitting of the kinetics data of fluoride sorption to the pseudo-second-order equation (Section 3.2). Thus, the sorption of fluoride on TM should be mainly by chemisorption (Daifullah et al. 2007).

3.8 Effect of Competing Anions

The interference of competing anions was investigated by varying the concentration of anions from 10 to 500 mg/L under 10 mg/L fluoride concentration at pH ~ 7. The results of the effects of co-existing anions on the adsorption of fluoride on TM are graphically presented in Fig. 9. It was noted that the presence of carbonate and phosphate ions in the solution in the concentration range of 100–500 mg/L significantly decreased fluoride removal, whereas the removal of fluoride slightly increased with the increase in the concentration of chloride, nitrate, and sulfate. The decrease in the removal of fluoride in the presence of

Table 3 Isotherm parameters of the equilibrium adsorption of fluoride on TM

Freundlich		Langmuir		Dubinin–Radushkevich	
Parameters	Value	Parameters	Value	Parameters	Value
K_F (L/g)	0.32	Q_{max} (mg/g)	1.56	q_m (mg/g)	2.70
n	2.70	b (L/mg)	0.14	E_{DR} (kJ/mol)	11.62
R^2	0.946	R_L	0.05–0.76	R^2	0.968
χ^2	0.21	R^2	0.949	χ^2	0.09
		χ^2	1.18		

carbonate and phosphate could be due to the high affinity of the adsorbent for carbonate and phosphate ions, and their competition for active binding sites with fluoride (Chen et al. 2010b). Fortunately, carbonate and phosphate ions are absent or very little in most groundwater sources of the Main Ethiopian Rift (Rango et al. 2010; Furi et al. 2011). Bicarbonate ion in the concentration range of 100–500 mg/L decreased the removal efficiency to a lesser extent, which could be due to a slight increase in the pH (Maiti et al. 2011). The inner-sphere and outer-sphere surface complexations of ion can be distinguished indirectly via the examination of the effect of ionic strength on the degree of adsorption (Hayes et al. 1988). Previous studies show that the uptake of target sorbate exhibits either no ionic strength dependence or increasing adsorption with increasing ionic strength when the sorbate adsorbs by inner-sphere complexation mechanism (Goldberg and Johnstony 2001; Mahmood et al. 2012). Similarly,

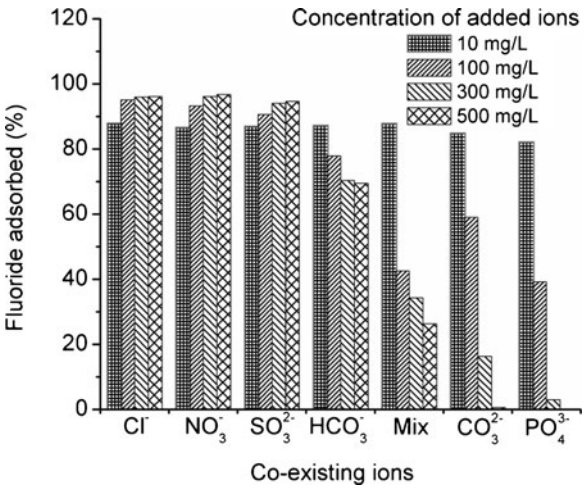

Fig. 9 Effect of competing ions on the efficiency of fluoride removal ($[F^-]_{initial}$, 10 mg/L; dose, 30 g/L; $pH_{initial}$, ~7; grain size, <0.075 mm; volume of solution, 0.5 L; contact time, 60 min; and shaking speed, 200 rpm)

the study conducted by McBride et al. (1997) demonstrates that the uptake of an anion that adsorbs by inner-sphere complexation either not suppressed by competition with weakly bonding anions such as chloride and nitrate or respond to the higher concentration of the weakly bonding anions with greater adsorption. As it can be seen from Fig. 9, the adsorption of fluoride on TM slightly increased with the increase in the concentration of chloride, nitrate, and sulfate ions (10–500 mg/L) in the solution. Thus, the little increase in the adsorption of fluoride on TM with the increase in the concentration of nitrate, chloride, and sulfate ions in the solution could substantiate the inner sphere complexation (chemisorption) of fluoride ions on TM that has been deduced from the value of the mean sorption energy, E_{DR} = 11.62 kJ/mol, computed from the D–R model (Table 3). A similar result has been observed by Maiti et al. (2011) for the removal of fluoride by chemical-treated laterite. In the presence of all the six anions in the same solution, the effect of carbonate and phosphate ions on the adsorption of fluoride became lesser possibly due to the buffering effects of the other ions. The overall influence of the co-existing anions on the adsorption of fluoride on TM followed the order: phosphate > carbonate > mixture > bicarbonate > sulfate $\approx$ nitrate $\approx$ chloride. The results of the effects of the studied competing anions are similar to the observation made by Chen et al. (2011a) for the removal of fluoride by porous granular ceramic-containing dispersed aluminum and iron oxides.

3.9 Removal of Fluoride from Natural Groundwater

Samples of natural groundwater respectively containing 7.56 and 15.93 mg/L fluoride were collected from two wells in the Main Campus of Jimma University, Ethiopia. The physicochemical characteristics of the samples are given in Table 4. Defluoridation of the samples of

Table 4 Physicochemical characteristics of groundwater samples

Characteristic parameter	Well #1	Well #2
Conductivity (μS/cm)	12,170	1,215.00
Total hardness (mg/L, $CaCO_3$)	645.56	738.00
Carbonate (mg/L, CO_3^{2-})	Nil	Nil
Bicarbonate (mg/L, HCO_3^-)	623.45	764.94
Chloride (mg/L, Cl^-)	12.04	3.41
Nitrate (mg/L, NO_3^-)	17.12	0.20
Sulfate (mg/L, SO_4^{2-})	1.22	3.94
Phosphate (mg/L, PO_4^{3-})	Nil	0.12
Fluoride (mg/L, F^-)	15.93	7.56
Calcium (mg/L, Ca^{2+})	24.00	10.64
Magnesium (mg/L, Mg^{2+})	7.89	3.65
Sodium (mg/L, Na^+)	289.12	278.0
pH	7.94	7.87

groundwater was carried out in duplicate without adjusting the pH of the water samples using 30 g/L TM under identical experimental conditions of the equilibrium batch adsorption study. Fluoride concentration of Well #1, 15.95 mg/L, was reduced to 5.05 mg/L. The reduction signified the need for further treatment to reduce the 5.05-mg/L fluoride to below the permissible level, 1.5 mg/L. However, the 7.56-mg/L fluoride content of Well #2 was successfully reduced to 1.43 mg/L, which is below the WHO guideline value of fluoride in drinking water. The pH of the defluoridated water was nearly neutral. Hence, the adsorbent could be used for the treatment of groundwater containing ~8 mg/L fluoride without adjusting the pH.

3.10 Desorption of Fluoride and Regeneration of TM

To develop a cost-effective adsorbent for pollutant removal from aqueous environment, it is important that the adsorbent should be regenerated for reuse. The pH effect on the efficiency of fluoride adsorption on TM showed (Fig. 6) that fluoride adsorption capacity was very low at pH > 10, suggesting the possibility of desorbing adsorbed fluoride from the saturated TM using alkaline solution. Based on this, batch desorption of ~90 % fluoride adsorbed was carried out under identical experimental conditions of the batch sorption studies (Section 2.4) using 500 mL of CES, 0.1 and 0.2 M NaOH solution separately. The percentages of fluoride desorbed at pH > 12 using CES, 0.1 and 0.2 M NaOH solutions were 79.87 %, 82.97 %, and 98.89 %, respectively (Fig. 9). Consequently, fluoride-loaded TM could be successfully regenerated using CES or NaOH solution. The mechanism of fluoride desorption from the saturated TM can be suggested in terms of the ligand exchange mechanism as depicted in Eq. 19.

$$\equiv \mathrm{MF} + \mathrm{OH}^- \leftrightarrow \equiv \mathrm{MOH} + \mathrm{F}^- \quad (19)$$

After desorbing fluoride from the fluoride-loaded TM, TM was rinsed with 0.1 M HCl until the pH of the supernatant solution was ~5, and fluoride readsorption study was conducted afterward. Fluoride readsorption results (Fig. 10) showed that fluoride adsorption efficiency of 86.00 %, 88.63 %, and 91.06 % were achieved, respectively, with the spent TM regenerated with CES, 0.1 and 0.2 M NaOH solution. The adsorption efficiencies of CES and 0.1 M NaOH regenerated TM were found to be slightly inferior to that of the fresh TM by 4.87 % and 1.97 %, respectively. However, the adsorption efficiency of TM regenerated using 0.2 M NaOH solution was similar to the adsorption efficiency of the fresh TM. It is important to note that the spent TM subjected to any of the desorbent used for the desorption of fluoride was competent to reduce 10 mg/L fluoride to below 1.5 mg/L after rinsing with 0.1 M HCl solution.

The loss of iron and aluminum from TM during desorption was investigated by analyzing the concentration of iron and aluminum in the supernatant solution after shaking the adsorbent at 200 rpm for 60 min at pH 12.81. It was found that 0.01 % iron and 0.70 %

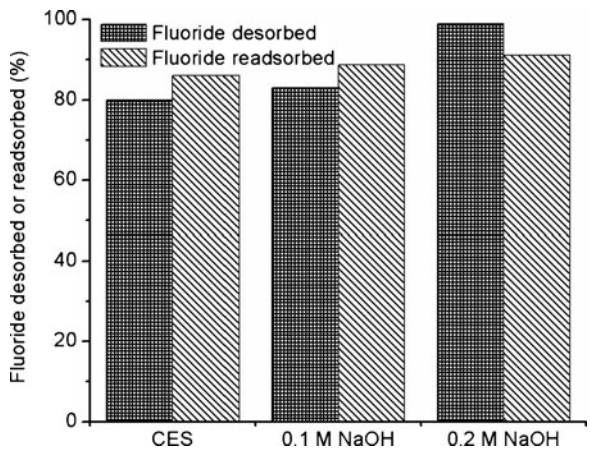

Fig. 10 Quantity of fluoride desorbed and adsorbed during the adsorption–desorption–adsorption cycle ($[F^-]_{initial}$, 10 mg/L; volume of solution, 0.5 L; contact time, 60 min; and shaking speed, 200 rpm)

aluminum, which together constituted <1 %, were released from the adsorbent, indicating that the loss of iron and aluminum from the adsorbent during regeneration was negligible. It was also observed that no detectable fluoride was released from the fluoride-loaded TM at pH ~ 5.0. The results of the adsorption–desorption–adsorption cycle showed that the fluoride-loaded TM can be either regenerated using CES or NaOH solution for reuse with insignificant loss of metals or safely disposed at pH ≤ 5.0. However, further investigation will be required to determine the exact life cycle of the regenerated TM.

4 Conclusions

The present study demonstrated the adsorption efficiency of locally available TM, containing mainly aluminum, iron, silicon, and titanium oxides, for fluoride removal from synthetic aqueous solution as well as groundwater samples. The adsorption of fluoride was rapid in the first 5 min at which ~87 % fluoride was removed, and equilibrium was attained within 10 min within which ~90 % adsorption efficiency was achieved. A high percentage (~90 %) of fluoride removal was obtained within a wide pH range of 3–8, which is of great importance in practical application. The broad optimum pH range could be attributed to the amphoteric nature of oxides of aluminum and iron. The kinetics of fluoride adsorption followed the pseudo-second-order equation with the coefficient of determination, $R^2 > 0.99$. The equilibrium adsorption of fluoride was most satisfactorily described by the D–R isotherm model ($R^2 = 0.968$, $\chi^2 = 0.09$), giving a sorption capacity of 2.70 mg/g. The computed value of the mean free energy of adsorption (E_{DR} = 11.62 kJ mol^{-1}) and the fitting of the adsorption kinetics data to the pseudo-second-order model ($R^2 >$ 0.99) could suggest that the sorption of fluoride on TM should be mainly by chemisorption. Fluoride adsorption was significantly reduced in the presence of carbonate, phosphate, and a mixture of co-existing anions, whereas slightly increased in the presence of chloride, nitrate, and sulfate ions. The overall influence of competing anions on the efficiency of fluoride removal by TM followed the order: phosphate > carbonate > mixture > bicarbonate > sulfate ≈ nitrate ≈ chloride. Thirty grams of TM per liter (30 g/L) successfully reduced 7.56 mg/L fluoride concentration of the groundwater sample to 1.43 mg/L, below the guideline value of 1.5 mg/L, without adjusting the pH. This demonstrates that the adsorbent could be used for defluoridation of groundwater containing ~8 mg/L fluoride. The adsorption–desorption–adsorption studies showed that fluoride-loaded TM can be regenerated without significant loss of metals using CES or NaOH solution for effective reuse, or can be safely disposed at pH ≤ 5.0. The fluoride removal efficiency of the regenerated fluoride-loaded TM was comparable to the fresh TM. Since the dissolution of the minerals was insignificant at neutral pH, TM could be used safely. Therefore, the results of the study could provide fundamental information to evaluate TM for the practical defluoridation of drinking groundwater.

Acknowledgments The first author is thankful to the Ethiopian Engineering Capacity Building Program (ECBP) and the German Academic Exchange Service (DAAD) for their financial support.

References

Abdulrahman, A. (1990). *Foraging activity and control of termites in western Ethiopia*. PhD thesis. London: University of London.

Abdus-Salam, N., & Itiola, A. D. (2012). Potential application of termite mound for adsorption and removal of Pb(II) from aqueous solutions. *Journal of the Iranian Chemical Society, 9*, 373–382.

Appel, C., & Ma, L. Q. (2002). Concentration, pH, and surface charge effects on Cd and Pb sorption in three tropical soils. *Journal of Environmental Quality, 31*, 581–589.

Appel, C., Lena, Q., Ma, R., Rhue, D., & Kennelle, E. (2003). Point of zero charge determination in soils and minerals via traditional methods and detection of electroacoustic mobility. *Geoderma, 113*, 77–97.

Ayoob, S., & Gupta, A. K. (2009). Performance evaluation of alumina cement granules in removing fluoride from natural and synthetic waters. *Chemical Engineering Journal, 150*, 485–491.

Balázsi, C., Kövér, Z., Horváth, E., Németh, C., Kasztosky, Z., Kurunczi, S., et al. (2007). Examination of calcium-phosphates prepared from eggshell. *Material Science Forum, 537–538*, 105–112.

Bhatnagar, A., Kumar, E., & Sillanpää, M. (2011). Fluoride removal from water by adsorption—a review. *Chemical Engineering Journal, 171*, 811–840.

Biswas, K., Gupta, K., & Ghosh, U. C. (2009). Adsorption of fluoride by hydrous iron(III)-tin(IV) bimetal mixed oxide from the aqueous solutions. *Chemical Engineering Journal, 149*, 196–206.

Brown, G. E., Henrich, V. E., Casey, W. H., Clark, D. L., Eggleston, C., Felmy, A., et al. (1998). Metal oxide

surfaces and their interactions with aqueous solutions and microbial organisms. *Chemical Reviews, 99*, 77–174.

Camacho, L. M., Torres, A., Saha, D., & Deng, S. (2010). Adsorption equilibrium and kinetics of fluoride on sol–gel-derived activated alumina adsorbents. *Journal of Colloid and Interface Science, 349*, 307–313.

Chauhan, V. S., Dwivedi, P. K., & Iyengar, L. (2007). Investigations on activated alumina based domestic defluoridation units. *Journal of Hazardous Materials, 139*, 103–107.

Chen, N., Zhang, Z., Feng, C., Li, M., Zhu, D., Chen, R., et al. (2010a). An excellent fluoride sorption behavior of ceramic adsorbent. *Journal of Hazardous Materials, 183*, 460–465.

Chen, N., Zhang, Z., Feng, C., Sugiura, N., Li, M., & Chen, R. (2010b). Fluoride removal from water by granular ceramic adsorption. *Journal of Colloid and Interface Science, 348*, 579–784.

Chen, N., Zhang, Z., Feng, C., Li, M., Zhu, D., & Sugiura, N. (2011a). Studies on fluoride adsorption of iron-impregnated granular ceramics from aqueous solution. *Materials Chemistry and Physics, 125*, 293–298.

Chen, N., Zhang, Z., Feng, C., Zhu, D., Yang, Y., & Sugiura, N. (2011b). Preparation and characterization of porous granular ceramic containing dispersed aluminum and iron oxides as adsorbents for fluoride removal from aqueous solution. *Journal of Hazardous Materials, 186*, 863–868.

Cornell, R. M., & Schwertmann, U. (1996). *The iron oxides: structure, properties, reactions, occurrence and uses*. New York: VCH.

Daifullah, A. A. M., Yakout, S. M., & Elreefy, S. A. (2007). Adsorption of fluoride in aqueous solutions using $KMnO_4$-modified activated carbon derived from stem pyrolysis of rich straw. *Journal of Hazardous Materials, 147*, 633–643.

Das, N., Pattanaik, P., & Das, R. (2005). Defluoridation of drinking water using activated titanium rich bauxite. *Journal of Colloid and Interface Science, 292*, 1–10.

DIN ISO 13878. (1998). *Bodenbeschaffenheit - Bestimmung des Gesamt-Stickstoffs durch trockene Verbrennung (Elementaranalyse)*. Berlin: Beuth.

DIN ISO 10 694. (1996). *Bodenbeschaffenheit-Bestimmung von organischem Kohlenstoff und Gesamtkohlenstoff nach trockener Verbrennung (Elementaranalyse)*. Berlin: Beuth.

Furi, W., Razack, M., Abiye, T. A., Ayenew, T., & Legesse, D. (2011). Fluoride enrichment mechanism and geospatial distribution in the volcanic aquifers of the Middle Awash basin, Northern Main Ethiopian Rift. *Journal of African Earth Sciences, 60*, 315–327.

Gergely, G., Wéber, F., Lukács, I., Tóth, A. L., Horváth, Z. E., Mihály, J., et al. (2010). Preparation and characterization of hydroxyapatite from eggshell. *Ceramics International, 36*, 803–806.

Goldberg, S., & Johnstony, C. T. (2001). Mechanisms of arsenic adsorption on amorphous oxides evaluated using macroscopic measurements, vibrational spectroscopy, and surface complexation modeling. *Journal of Colloid and Interface Science, 234*, 204–216.

Guo, H., Stüben, D., & Berner, Z. (2007). Removal of arsenic from aqueous solution by natural siderite and hematite. *Applied Geochemistry, 22*, 1039–1051.

Hayes, K. F., Papelis, C., & Leckie, J. O. (1988). Modeling ionic strength effects on anion adsorption at hydrous oxide/solution interface. *Journal of Colloid and Interface Science, 125*, 717–726.

Ho, Y. S., & McKay, G. (1999). Pseudo-second-order model for sorption process. *Process Biochemistry, 34*, 451–465.

Jagtap, S., Thakre, D., Wanjari, S., Kamble, S., Labhsetwar, N., & Rayalu, S. (2009). New modified chitosan-based adsorbent for defluoridation of water. *Journal of Colloid and Interface Science, 332*, 280–290.

Jagtap, S., Yenkie, M. K., Labhsetwar, N., & Rayalu, S. (2012). Fluoride in drinking water and defluoridation of water. *Chemical Reviews, 112*, 2454–2466.

Jouquet, P., Mamou, P., Lepage, M., & Velde, B. E. (2002). Effect of termite on clay minerals in tropical soils: fungus-growing termites as weathering agents. *European Journal of Soil Science, 53*, 521–527.

Kaufhold, S., Dohrmann, R., Abidin, Z., Henmi, T., Matsue, N., Eichinger, L., et al. (2010). Allophane compared with other sorbent minerals for the removal of fluoride from water with particular focus on a mineable Ecuadorian allophane. *Applied Clay Science, 50*, 23–33.

Kumar, E., Bhatnagar, A., Ji, M., Jung, W., Lee, S.-H., Kim, S.-J., et al. (2009). Defluoridation from aqueous solutions by granular ferric hydroxide (GFH). *Water Research, 43*, 490–498.

Liu, C., & Evett, J. B. (2003). *Soil properties—testing, measurement, and evaluation. ISBN: 0-13-093005-9*. USA: Banta Book Company.

Liu, Q., Guo, H., & Shan, Y. (2010). Adsorption of fluoride on synthetic siderite from aqueous solution. *Journal of Fluorine Chemistry, 131*, 635–641.

Lopez-Hernandez, D., Brossard, M., Fardeau, J. C., & Lepage, M. (2006). Effect of different termite feeding groups on P sorption and P availability in African and South American savannas. *Biology and Fertility of Soils, 42*, 207–214.

Lucy, M. C., Arely, T., Dipendu, S., & Shuguang, D. (2010). Adsorption equilibrium and kinetics of fluoride on sol–gel-derived activated alumina adsorbents. *Journal of Colloid and Interface Science, 349*, 307–313.

Mahmood, T., Din, S. U., Naeem, A., Mustafa, S., Waseem, M., & Hamayun, M. (2012). Adsorption of arsenate from aqueous solution on binary mixed oxide of iron and silicon. *Chemical Engineering Journal, 192*, 90–98.

Maiti, A., Basu, J. K., & De, S. (2011). Chemical treated laterite as promising fluoride adsorbent for aqueous system and kinetic modeling. *Desalination, 265*, 28–36.

Maliyekkal, S. M., Shukla, S., Philip, L., & Nambi, I. M. (2008). Enhanced fluoride removal from drinking water by magnesia-amended activated alumina granules. *Chemical Engineering Journal, 140*, 183–192.

McBride, M. B. (1997). A critique of diffuse double layer models applied to colloid and surface chemistry. *Clays and Clay Minerals, 45*, 598–608.

Meenakshi, S., Sundaram, C. S., & Sukumar, R. (2008). Enhanced fluoride sorption by mechanochemically activated kaolinites. *Journal of Hazardous Materials, 153*, 164–172.

Mohapatra, M. S., Anand, S., Mishra, B. K., Giles, D. E., & Singh, P. (2009). Review of fluoride removal from drinking water. *Journal of Environmental Management, 91*, 67–77.

Nigussie, W., Zewge, F., & Chandravanshi, B. S. (2007). Removal of excess fluoride from water using waste residue

from alum manufacturing process. *Journal of Hazardous Materials, 147*, 954–963.

OADB (2001). *Phase II*: *Integrated pilot project for termite control in 8 districts of East and West Wellega Zone*, *Oromia*. Finfinnee: Oromia Agricultural Development Bureau (OADB).

Ramos, L. R., Utrilla, R. J., Castillo, N. M., & Polo, M. S. (2010). Kinetic modeling of fluoride adsorption from aqueous solution onto bone char. *Chemical Engineering Journal, 158*, 458–467.

Rango, T., Bianchini, G., Beccaluva, L., & Tassinari, R. (2010). Geochemistry and water quality assessment of central Main Ethiopian Rift natural waters with emphasis on source and occurrence of fluoride and arsenic. *Journal of African Earth Sciences, 57*, 479–491.

Sakhare, N., Lunge, S., Rayalu, S., Bakardjiva, S., Subrt, J., Devotta, S., et al. (2012). Defluoridation of water using calcium aluminate material. *Chemical Engineering Journal, 203*, 406–414.

Sarı, A., & Tuzen, M. (2009). Biosorption of As(III) and As(V) from aqueous solution by macrofungus (*Inonotus hispidus*) biomass: equilibrium and kinetic studies. *Journal of Hazardous Materials, 164*, 1372–1378.

Sarkar, M., Banerjee, A., Pramanick, P. P., & Sarkar, A. R. (2006). Use of laterite for the removal of fluoride from contaminated drinking water. *Journal of Colloid and Interface Sciences, 302*, 432–441.

Semhi, K., Chaudhuri, S., Claurer, N., & Boeglin, J. L. (2008). Impact of termite activity on soil environment: a perspective from their soluble chemical components. *International journal of Environmental Science and Technology, 5*, 431–444.

Shriver, D. F., Atkins, P. W., & Langford, C. H. (1994). *Inorganic chemistry*. Oxford: Oxford University Press.

Solangi, I. B., Memon, S., & Bhanger, M. I. (2009). Removal of fluoride from aqueous environment by modified Amberlite resin. *Journal of Hazardous Materials, 171*, 815–819.

Sujana, M. G., & Anand, S. (2010). Iron and aluminium based mixed hydroxides: a novel sorbent for fluoride removal from aqueous solutions. *Applied Surface Science, 256*, 6956–6962.

Sujana, M. G., Thakur, R. S., & Rao, S. B. (1998). Removal of fluoride from aqueous solution by alum sludge. *Journal of Colloid and Interface Science, 206*, 94–101.

Tadesse, S., Milesi, J.-P., & Deschamps, Y. (2003). Geology and mineral potential of Ethiopia: a note on geology and mineral map of Ethiopia. *Journal of African Earth Sciences, 36*, 273–313.

Thakre, D., Rayalu, S., Kawade, R., Meshram, S., Subrt, J., & Labhsetwar, N. (2010). Magnesium incorporated bentonite clay for defluoridation of drinking water. *Journal of Hazardous Materials, 180*, 122–130.

Thole, B. (2011). Defluoridation kinetics of 200 °C calcined bauxite, gypsum, and magnesite and breakthrough characteristics of their composite filter. *Journal of Fluorine Chemistry, 132*, 529–535.

Thongthai, W. (2011). Characterization of calcium oxide derived from waste eggshell and its application as CO_2 sorbent. *Ceramics International, 37*, 3291–3298.

Tian, Y., Wu, M., Liu, R., Wang, D., Lin, X., Liu, W., et al. (2011). Modified native cellulose fibers: a novel efficient adsorbent for both fluoride and arsenic. *Journal of Hazardous Materials, 185*, 93–100.

Tilahun, A., Kebede, F., Yamoah, C., Erens, H., Mujinya, B. B., Verdoodt, A., et al. (2012). Quantifying the masses of *Macrotermes subhyalinus* mounds and evaluating their use as a soil amendment. *Agriculture, Ecosystems and Environment, 157*, 54–59.

Tor, A., Danaoglu, N., Arslan, G., & Cengeloglu, Y. (2009). Removal of fluoride from water by using granular red mud: batch and column studies. *Journal of Hazardous Materials, 164*, 271–278.

Tripathy, S. S., & Raichur, A. M. (2008). Abatement of fluoride from water using manganese dioxide-coated activated alumina. *Journal of Hazardous Materials, 153*, 1043–1051.

Wang, Y., & Reardon, E. J. (2001). Activation and regeneration of a soil sorbent for defluoridation of drinking water. *Applied Geochemistry, 16*, 531–539.

WHO. (2006). *Guidelines for drinking water quality. First addendum to 3rd edition. Vol. 1: Recommendations*. Geneva: World Health Organization.

Zhao, Y., Li, X., Liu, L., & Chen, F. (2008). Fluoride removal by Fe(III)-loaded ligand exchange cotton cellulose adsorbent from drinking water. *Carbohydrate Polymers, 272*, 144–150.